Active Site Mapping of *Escherichia coli* D-Ala-D-Ala Ligase by Structure-Based Mutagenesis†

Yian Shi and Christopher T. Walsh*

Department of Biological Chemistry and Molecular Pharmacology, Harvard Medical School, 240 Longwood Avenue, Boston, Massachusetts 02115

Received October 3, 1994; Revised Manuscript Received December 16, 1994®

ABSTRACT: Eleven *Escherichia coli* D-Ala-D-Ala ligase (DdlB) mutants, at K144, K215, and E270 in the ATP binding site, at E15, S150, H63, and R255 in the first D-Ala subsite, and at Y216, S281, L282, and D257 in the second D-Ala subsite, were constructed, purified, and examined for steady-state kinetic parameters, k_{cat} and K_ms for ATP, and both first (D-Ala_1), and second (D-Ala_2) D-alanines. Of these, E270Q, K215A, R255A, and D257N retained very low or no detectable activity consistent with X-ray structure based predictions for roles in Mg^{2+} coordination to β,γ-P of ATP (E270), coordination to transferring γ-PO_3 of ATP (K215), and coordination/orientation of nucleophilic COO^- of D-Ala_1 that attacks γ-PO_3 of ATP (R255, D257) and the side chain of R255, respectively. The substantial retention of activity in the Y216F mutant argues against the possibility that Y216 may be a catalytic base that deprotonates the α-NH_3^+ of D-Ala_2 to attack the acyl phosphate form of D-Ala_1. While all seven mutants that retain activities have a 300−2000 fold elevation in K_m for D-Ala_1 (1−2 μM in wild type), the S281A mutant has a 500-fold elevation in K_m for D-Ala_2, consistent with a proposed interaction with the COO^- of D-Ala_2. Similarly, the kinetics of inhibition by a slow-binding phosphinate inhibitor in the presence of ATP are most altered in the S281A mutant.

The peptidoglycan (PG)[1] layer of the bacterial cell wall is an essential structure that confers resistance to osmotic lysis of bacteria. Covalent connections of adjacent peptide strands in the PG layer provide the tensile strength to this marcomolecular meshwork, and several antibacterial agents exert their effects by blockade of cross-linking steps (β-lactams, vancomycin) (Waxman, 1983; Wihelm, 1991) or inhibition of precursor synthesis (e.g., fosfomycin, D-cycloserine) (Kahan, 1974; Pitillo, 1953). Among the enzymes of consequence in the PG biosynthetic pathway are those generating and utilizing D-alanine-containing molecules. The dipeptide D-Ala-D-Ala is a central structure in the pathway, generated from the consecutive action of alanine racemase and the ATP-dependent amide bond forming D-Ala-D-Ala ligase (Ddl) (eq 1) (Wright & Walsh, 1992). D-Ala-

$$\text{D-Ala}_1 + \text{D-Ala}_2 + \text{ATP} \xrightarrow{\text{Ddl}} \text{D-Ala}_1\text{-D-Ala}_2 + \text{ADP} + \text{P}_i \quad (1)$$

D-Ala is then added to the terminus of a UDP-muramyl tripeptide to produce the pentapeptide product with an N-acylated D-Ala-D-Ala terminus (Walsh, 1989). After translocation from the cytoplasmic face to the periplasmic face of the membrane the D-Ala-D-Ala moiety of the pentapeptide is an important recognition determinant in the action of β-lactam and of glycopeptide antibiotics. The covalent cross-linking of one PG peptide strand to another and the concomitant generation of mechanical strength involve enzymatic transpeptidation with attack of the ϵ-NH_2 of a Lys or diaminopimelate (DAP) residue at position 3 on one strand at the penultimate D-Ala (position 4) on another strand, with release of the terminal D-Ala as the free amino acid. These transpeptidases are killing sites of penicillins and cephalosporins (Gale et al., 1981). Prior to transpeptidative cross-linking, the N-acylated D-Ala-D-Ala pentapeptide terminus can function as a high-affinity site for vancomycin, whose binding will occlude subsequent action of the transpeptidase and thus yield a defective under-cross-linked PG layer (Bugg & Walsh, 1992).

We have been investigating the enzymes of the D-alanine pathway for some time (Walsh, 1989) with particular attention to the D-Ala-D-Ala-forming ligase (Ddl) of eq 1. It is the site of action of the antibiotic D-cycloserine (Daub et al., 1988) and has gained special recent interest because, in the case of clinical resistance to vancomycin, a *ddl* homologue termed the *vanA* gene encodes an enzyme that makes the depsipeptide D-Ala-D-lactate rather than D-Ala-D-Ala (Dukta-Malen et al., 1990; Bugg et al., 1991a,b). In resistant bacteria vancomycin has a 1000-fold lower affinity for PG structures terminating in D-Ala-D-lactate (Bugg et al., 1991b) rather than D-Ala-D-Ala, accounting for the observed clinical phenotype. Thus, there is much interest in deciphering not only the structure/function aspects of D-Ala-D-Ala ligase but also the differences that enable VanA to have gained the catalytic capacity to activate D-lactate and produce the unique D-Ala-D-lactate depsipeptide product.

We have intensively studied *Escherichia coli* Ddl, including cloning of a second gene, DdlA and DdlB, overproduction, purification, and mechanistic analysis (Daub et al., 1988;

† This work was supported in part by NSF Grant DMB 8917290 and NIH Grant GM 49338-01.

* Author to whom correspondence should be addressed.

® Abstract published in *Advance ACS Abstracts,* February 1, 1995.

[1] Abbreviations: BSA, bovine serum albumin; Ddl, D-Ala-D-Ala ligase; EDTA, ethylenediaminetetraacetic acid; HEPES, 4-(2-hydroxyethyl)-1-piperazineethanesulfonic acid; IPTG, isopropyl thiogalactoside; PCR, polymerase chain reaction; PG, peptidoglycan; PEP, phosphoenolpyruvate; NADH, reduced nicotinamide adenine dinucleotide; LDH, lactate dehydrogenase; PK, pyruvate kinase.

0006-2960/95/0434-2768$09.00/0

Zawadzke et al., 1991). We have similarly overproduced, purified, and analyzed VanA (Bugg et al., 1991a,b) and VanB (Shi and Walsh, unpublished data) from expression constructs in *Escherichia coli*. One of the most useful approaches to study the catalytic mechanism of these ligases and to explore inhibition has been the analysis of time-dependent inactivation of Ddl by a phosphinate analog **1** of D-Ala-D-Ala in the

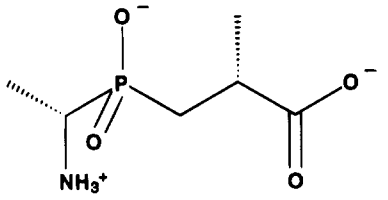

1

presence of ATP (Parsons et al., 1988). The ligase catalyzes γ-PO_3 transfer from ATP to the oxygen of the phosphinate **1** to yield a phosphinophosphate **2**−ADP complex that mimics a tetrahedral reaction intermediate that would arise in normal catalysis from attack of D-Ala_2 on the acyl phosphate which was generated from the attack of D-Ala_1 on ATP (eq 2). The phosphinophosphate complex binds so

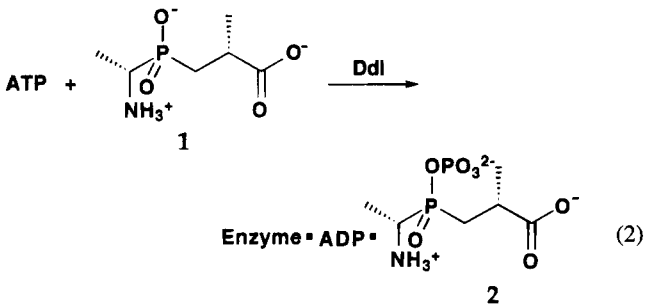

(2)

2

tightly that it dissociates over a period of many hours to days, leading to enzyme inactivation by slow-binding inhibition (Duncan et al., 1988, 1989; McDermott et al., 1990). We have observed that *E. coli* DdlB crystallizes in the presence of ATP and phosphinate **1** and have recently determined the X-ray structure of the enzyme−ADP−phosphinophosphate complex (Fan et al., 1994). The structure reveals an ω-loop which closes over the two bound small molecules (Figure 1a) and allows definition of the active site region of the ligase, including subsites for binding of ATP, D-Ala_1, and D-Ala_2 (Figure 1b). The structure of this stable ligase−phosphinophosphate inactivation complex has led to predictions about the possible roles of specific amino acid side chains in substrate binding and catalysis, including how Ddl and the 30% homologous VanA may make identical acyl phosphate from D-Ala_1 but differentially activate D-Ala_2 or D-lactate as the nucleophilic cosubstrate.

In this work we report construction of 11 Ddl mutants, their overproduction, purification to homogeneity, and characterization of steady-state kinetic constants. We have also tested a subset for slow-binding inhibition by phosphinate **1**. These results test several predictions from the X-ray structure.

MATERIALS AND METHODS

ATP, D-Ala, and phosphoenolpyruvate (PEP) were purchased from Sigma. 4-(2-Hydroxyethyl)-1-piperazineethanesulfonic acid (HEPES), reduced nicotinamide adenine dinucleotide (NADH), lactate dehydrogenase (LDH), and pyruvate kinase (PK) were from Boehringer Mannheim Biochemicals. Restriction endonucleases and other DNA-modifying enzymes were purchased from New England Biolabs. Oligonucleotide primers were synthesized by the BCMP facility (Harvard Medical School). The inhibitor [1(*S*)-aminoethyl]-[2-carboxy-2(*R*)-methyl-1-ethyl]phosphinic acid was a generous gift of Drs. B. Ellsworth and P. A. Bartlett, University of California, Berkeley.

Site-Directed Mutagenesis. The site-directed mutagenesis was accomplished by using either one-round or two-round (megaprimer) polymerase chain reaction (PCR) (Sarkar & Sommer, 1990). The sequences of the PCR products were confirmed by dideoxy sequencing. In all cases, plasimid pTB_2 (a pKK-223-3 vector containing *ddl* gene) was used as template (Zawadzke et al., 1991). The oligonucleotide primers used are as follows (the bases encoding the new amino acid are in boldface): primer 1 (E15Q), 5′-CAGAGAAACTTCCCG**CTG**AGCGGAGGTCCCACC; primer 2 (H63Q), 5′-CTCGAGCATCCCCTGCAGCGTACCATCTTCACCGCCGCGACCC**TG**TAGCGCGATAAACAC; primer 3 (K144A), 5′-CCGGTTATCGTT**GCG**CCGAGCCGCGA; primer 4 (K144T), 5′-CCGGTTATCGTT**ACG**CCGAGCCGCGA; primer 5 (S150A), 5′-CCGCGAAGGT**GCC**AGTGTGGG; primer 6 (K215A), 5′-ATTCAACCGTCCGGAACCTTCTATGATTATGAGGCG**GCA**TATCTCTCTGATGAGACACAG; primer 7 (K215E), 5′-ATTCAACCGTCCGGAACCTTCTATGATTATGAGGCG**GAG**TATCTCTCTGATGAGACACAG; primer 8 (K215R), 5-ATTCAACCGTCCGGAACCTTCTATGATTATGAGGCG**AGA**TATCTCTCTGATGAGACACAG; primer 9 (K215E/Y216K), 5′-ATTCAACCGTCCGGAACCTTCTATGATTATGAGGCGGAAAAACTCTCTGATGAGACACAGTAT; primer 10 (Y216F), 5′-ATTCAACCGTCCGGAACCTTCTATGATTATGAGGCGAAGTTTCTCTCTGATGAGACACAG; primer 11 (Y216K), 5-ATTCAACCGTCCGGAACCTTCTATGATTATGAGGCGAAG**AAA**CTCTCTGATGAGACACAG; primer 12 (D257N), 5′-GGATGGGGACGTATTAACGTTATGCTGGACAGCGAT; primer 13 (E270Q), 5′-TTTTATCTGCTG**CAA**GCCAATACC; primer 14 (S281-A), 5′-CCGGGTATGACCAGCCAC**GCA**CTGGTGCCGATGGCGGCA; primer 15 (L282R), 5′-ATGACCAGCCACAGC**AGA**GTGCCGATGGCGGCA; primer 16 (5′-primer), 5′-GCATGCTCTAGAAGGAGATATACATATG; primer 17 (5′-primer), 5′-GGCGGTATTGACGCGTATCCTGTC; primer 18 (5′-primer), 5′-AGTGATGGCATCTGCGCTTTC; primer 19 (5′-primer), 5′-ACACAGTATTTCTGCCCCGCA; primer 20 (3′-primer), 5′-ACTTTCTGAAAGCCCATCGACTTC; primer 21 (3′-primer), 5′-CGTAGCAAGCTTTTAGTCCGCCAGTTCCAGAATTCG. Mutants H63Q, K215A, K215E, K215R, K215E/Y216K, Y216F, and Y216K were constructed by one-round PCR. H63Q was made by ligating the *Mlu*I−*Pst*I-digested PCR product of primers 17 and 2 into the *Mlu*I−*Pst*I linearized pTB_2. In the cases of the K215 and Y216 mutants, primer 21 was used as the 3′-primer; primers 6, 7, 8, 9, 10, and 11 was used as 5′-primers, respectively. The resulting PCR products were digested by *Bsp*EI and *Hin*dIII and then ligated into the *Bsp*EI−*Hin*dIII linearized pTB_2 to give the desired constructs. All other mutants were constructed by two-round PCR. E15Q was constructed by ligating the *Xba*I−*Mlu*I-linearized pTB_2 and *Xba*I−*Mlu*I-digested PCR product made from primer 20 and the megaprimer (a product of primers 16 and 1). Mutants K144A, K144T, S150A, and E270Q were made by ligating

the *StuI*−*Hin*dIII-linearized pTB$_2$ and *StuI*−*Hin*dIII-digested PCR products of primer 18 and the corresponding megaprimers, made by using primer 21 as the 3′-primer and primers 3, 4, 5, and 13 as 5′-primers respectively. Mutants D257N, S281A, and L282R were made by ligating the *Bsp*EI−*Hin*dIII-linearized pTB$_2$ and *Bsp*EI−*Hin*dIII digested PCR products of primer 16 and the corresponding megaprimers, made by using primer 21 as the 3′-primer and primers 12, 14, and 15 as 5′-primers, respectively. All the constructs were transformed into *E. coli* strain W3110.

Overexpression and Purification of the Wild-Type and Mutant DdlB. The *E. coli* strain W3110 containing wild-type or mutant plasmid was grown at 37 °C in 1 L of LB containing ampicillin (100 μg/mL) to an A_{595} of about 0.6; at this point, IPTG was added to a final concentration of 1 mM to induce the *tac* promoter. Cells were then grown for a further 5−7 h at 37 °C and harvested by centrifugation at 5000 rpm for 10 min. The cell pellet was rapidly frozen in liquid nitrogen and stored at −70 °C. The proteins were purified as described (Zawadzke et al., 1991).

Kinetic Measurement and Analysis of the Wild-Type and Mutant DdlB. The kinetic assays on the purified proteins were carried out with the continuous ADP release coupled assay (Daub et al., 1988). The assay mixture contained the following components (final concentration): 100 mM HEPES (pH 7.8), 10 mM KCl, 10 mM $MgCl_2$, ATP (see text for concentration), 2.5 mM PEP, 0.15−0.2 mM NADH, 50 units/mL LDH, 50 units/mL PK, and D-Ala (see text for concentration). The assay was carried out at 37 °C and monitored at 340 nm. The kinetic analysis was carried out as described previously (Neuhaus, 1962a,b; Zawadzke et al., 1991). Applying the steady-state approximation, a rate equation (eq b) could be obtained on the basis of the proposed reaction sequence as shown in eq a. V_{max} could be obtained from either eq b or eq c by curve fitting. With the resultant V_{max} value, a subsequent plot of [S]($1/V - 1/V_{max}$) against 1/[S] gave a straight line (eq d), whose y intercept (K_2/V_{max}) and slope (K_1K_2/V_{max}) provided the two K_m values.

$$E + S \overset{K_1}{\rightleftharpoons} ES + S \overset{K_2}{\rightleftharpoons} ES_2 \xrightarrow{k_{cat}} E + P \qquad (a)$$

$$V = \frac{V_{max}[S]^2}{K_1K_2 + K_2[S] + [S]^2} \qquad (b)$$

$$\frac{1}{V} = \frac{1}{V_{max}} + \frac{K_2}{V_{max}}\frac{1}{[S]} + \frac{K_1K_2}{V_{max}}\frac{1}{[S]^2} \qquad (c)$$

$$[S]\left(\frac{1}{V} - \frac{1}{V_{max}}\right) = \frac{K_2}{V_{max}} + \frac{K_1K_2}{V_{max}}\frac{1}{[S]} \qquad (d)$$

Slow-Binding Inhibition Studies. The inhibitory effect of (aminoalkyl)phosphinate on the wild-type and mutant DdlBs was studied by the PK-LDH coupled assay and analyzed by reported procedures (Morrison & Walsh, 1988; Duncan & Walsh, 1988). A series of progress curves were obtained at different concentrations of inhibitor. The rate of approach to steady state, k_{obsd}, was determined by measuring the reaction velocity (v) at various times, initial velocity (v_o), and steady state velocity (v_s) from the progress curves. Based on eq e, a plot of $\ln[(v - v_s)/(v_0 - v_s)]$ *vs* t gave a line whose slope was equal to the apparent first-order rate constant $-k_{obsd}$. From the values of k_{obsd} obtained at various inhibitor concentrations, a net second-order inactivation rate constant, $k_{on}(k_{obsd}/[I])$ was calculated. k_{inact} and K_i' ($K_i' = K_i(1 + [S]/K_{m1})$ values were obtained by a plot of $1/k_{obsd}$ *vs* 1/[I] from eq f, derived on the basis of the reaction scheme as

$$v = v_s + (v_0 - v_s)\exp(-k_{obsd}t) \qquad (e)$$

$$k_{obsd} = k_4 + k_{inact}[I]/([I] + K_i') \qquad (f)$$

shown in eq 3 (see text). With known [S], an affinity ratio K_i/K_{m1} could be obtained (the assumption was made that $[S]/K_{m1}$ was much greater than 1).

Protein Determination. Protein concentrations were determined by the method of Bradford with bovine serum albumin as the standard (Bradford, 1976).

RESULTS

Selection and Production of Ddl Mutants. The recently reported X-ray structure of *E. coli* Ddl with bound ADP and phosphinophosphate **2** as a reaction intermediate analog (see Figure 1) (Fan et al., 1994) guided initial design for mutant construction to test for residue function. Of the several residues interacting with ADP (K97, K144, K215, E270, N272), we opted to mutate three, K144 (K144A, T), K215 (K215E, K215A, and in the double mutant K215E/Y216F), and E270 (E270Q), to probe for effects on catalytic efficiency. The phosphorylated tetrahedral phosphinate **2** has a set of eight side chains in its proximity (Figure 1b) that may be consequential for providing the interaction energy (K_i = 33 nM in wild-type enzyme) that makes it a slowly dissociating ($t_{1/2}$ = ca. 16 days) inhibitor and presumably also stabilize the normal tetrahedral adduct in catalysis. In the subsite that would correspond to D-Ala$_1$ recognition, the side chains of E15, H63, S150, and R255 are in proximity to **2**, while in the subsite for the D-Ala$_2$, the side chains of Y216, D257 (*via* a water molecule), S281, and L282 were possible participants in recognition and/or catalysis. The roles projected for each of the 11 active site residues seen in the X-ray structure are noted in Table 1, along with the subsites of the active site in which they may function. Also listed are the choices of side-chain replacement in each mutant that were prepared.

As detailed in Materials and Methods, each mutant was constructed by PCR mutagenesis, expressed in *E. coli* W3110 with overproduction and purified to homogeneity as previously reported for wild-type *E. coli* ddlB (Zawadzke et al., 1991). The range of overproduction varied from 100 to 150 mg/L, and purities were greater than 95% by SDS gel analysis. A possible complication to analysis arises from the fact that the DdlB mutants were expressed in a cell containing endogenous, low levels of both wild-type DdlA and DdlB, and even with high overproduction a certain level of contaminating wild-type enzyme activity (DdlA, DdlB, or both) would be present. A scan of Table 2 gives some sense of the scope of the signal to noise level and the lower limits of activity ascribable to a mutant Ddl. Overproduction of wild-type *E. coli* DdlB gave enzyme with a k_{cat} of 1870 min^{-1}, in close agreement with our previously published turnover numbers (Bugg et al., 1991a). The D257N mutant enzyme preparation had a k_{cat} of 0.18 min^{-1}, while the double mutant K215E/Y216K was 0.28 min^{-1} and a triple mutant K215E/Y216K/L282R (data not shown) was 0.5 min^{-1}. Also two loop replacement mutants (DdlB to VanA) (data not shown) were 0.4−0.7 min^{-1}. While these five mutants could

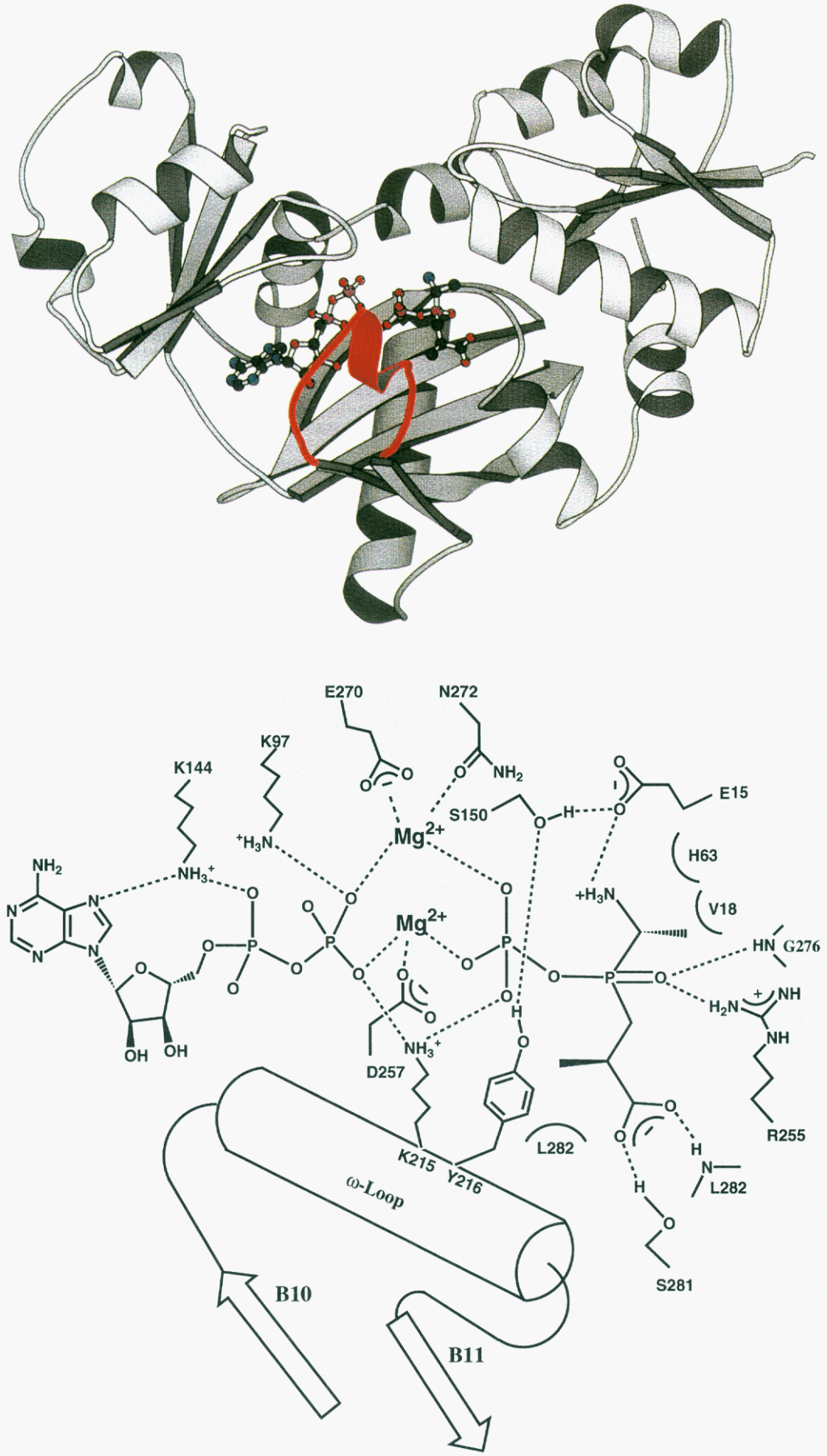

FIGURE 1: Global view of the complex of the *E. coli* D-Ala-D-Ala ligase with ADP and the phosphinophosphate transition-state analog **1**. The part in red is the ω-loop (residues 205−220). ADP and the phosphinophosphate are shown in stick-and-ball form, with ADP on the left and inhibitor **2** on the right. (b, bottom) Schematic diagram of the residues around ADP and phosphorylated phosphinate inhibitor **2**. The possible interactions are shown by dashed lines. Hydrogen bond distances in the triad Y216−S150 and S150−E15 are 2.8 and 2.6 Å, respectively. Residues K215 and Y216 are shown as part of the ω-loop (residues 205−220).

Table 1: *Escherichia coli* D-Ala-D-Ala Ligase Mutants to Probe Structure/Function Predictions

residues	mutant	proposed function from X-ray analysis	subsite
K144	K144A, T	coordination of N_7 and α-P of ATP	ATP
K215	K215E, A, R	coordination of γ-PO_3^{2-} group undergoing transfer	ATP
E270	E270Q	coordination of Mg^{2+} binding to β- and γ-P of ATP	ATP
E15	E15Q	H bond network to S150 and interaction with NH_3^+ of D-Ala_1	D-Ala_1
S150	S150A	H bond network to E15, Y216	D-Ala_1
H63	H63Q	proximity to amino and methyl group of D-Ala_1	D-Ala_1
R255	R255A	binding of D-Ala_1-COO^-, polarization, and charge stabilization	D-Ala_1
Y216	Y216F, K	H bond to S150, possible base for NH_3^+ of D-Ala_2	D-Ala_2
D257	D257N	(a) H bond to an H_2O molecule as possible base for NH_3^+ of D-Ala_2; (b) coordination to Mg^{2+} and salt bridge with R255	D-Ala_2, ATP
S281	S281A	binding of D-Ala_2-COO^-	D-Ala_2
L282	L282R	interaction with CH_3 side chain of D-Ala_2	D-Ala_2

Table 2: Steady-State Kinetic Parameters for Ddl Mutants

mutants	k_{cat} (min^{-1})	K_1(D-Ala)[a] (mM)	K_2(D-Ala)[a] (mM)	K_{cat}/K_2 (min^{-1} mM^{-1})	K_m(ATP)[b] (mM)
WT	1870	0.0012	1.13	1655	0.049
E15Q	686	0.43	43.7	15.7	0.055
H63Q	1565	0.55	57.5	27.2	0.161
K144A (5 mM ATP)	397	<0.1[c]	22.8	17.4	2.4
K144A (15 mM ATP)	504	<0.2[c]	22.9	22	
K144T (5 mM ATP)	151	<0.3[c]	70.3	2.14	2.5
K144T (15 mM ATP)	237	<0.3[c]	86	2.76	
S150A	2107	0.76	60.4	34.9	0.179
Y216F	1407	0.26	25.7	54.7	0.033
Y216K	~930	0.43	>105[d]	2.3	0.008
S281A	~1659		≫100[d]	0.46	<0.005[e] (~0.0012)
L282R	158	0.49	20.9	7.6	0.046
D257N	0.18		1.05		
E270Q	4.06		46		0.188
K215E/Y216K	0.28		1.29		
R255A	0.6				

[a] For the determination of kinetic parameters for D-Ala, usually 5 mM ATP was used unless specified. [b] For the determination of kinetic parameters for ATP, 80 mM D-Ala was used; K_ms were usually determined by varying [ATP] at 10 mM $MgCl_2$ except in the cases of K144A and K144T, where K_m values were determined by varying [ATP·Mg] with 10 mM $MgCl_2$ fixed. [c] The lowest [D-Ala] used. [d] The highest [D-Ala] used. [e] The lowest [ATP] used.

have real residual activities, it is likely that any number of 0.7 min^{-1} and below, while measurable, is instead residual wild-type enzyme, copurifying with mutants at an abundance level of less than or equal to 1part in 2000, 0.7 min^{-1}/1870 min^{-1}. A level of 1 part endogenous wild-type Ddl (B and A) to 2000 parts overexpressed DdlB mutant would give the dynamic range for interpretation in these studies. A further indication of this level of signal to wild-type noise could be obtained by analyzing K_m values for D-Ala_1 and D-Ala_2. Neuhaus initially reported deconvolution of the V *vs* S plots for D-Ala into distinct K_m values for D-Ala_1 and D-Ala_2 with Ddl from *Streptococcus faecalis* R (Neuhaus, 1962a) and we (Zawadzke et al., 1991) noted about a 300 fold difference in K_m values for D-Ala_1 (~3 μM) and D-Ala_2 (1 mM) with *E. coli* DdlB. In Table 2 we note that in these studies K_m for D-Ala_1 for wild-type DdlB is 1.2 μM and 1130 μM for D-Ala_2 for almost 3 orders of magnitude higher affinity by the K_{m1}/K_{m2} ratio for D-Ala_1/D-Ala_2. When a purified low specific activity mutant Ddl such as E270Q was examined, a *V/S vs V* plot (Figure 2) shows the data are well fit by two distinct slopes. The data shown as closed circles give a k_{cat} of 0.93 min^{-1} and a K_m of 2.8 mM (for D-Ala_2). The data in the open circles yield a K_m of 46 mM and a k_{cat} of 4.6 min^{-1}. The first set of data are most probably due to contaminating wild-type Ddl and the second due to intrinsic activity of E270Q Ddl. Similar analyses of mixtures of enzyme isoforms reported in Segel (1975) validate this interpretation and show that a 2−3-fold overestimate of K_m for the low k_{cat} form is common in this analysis. This further

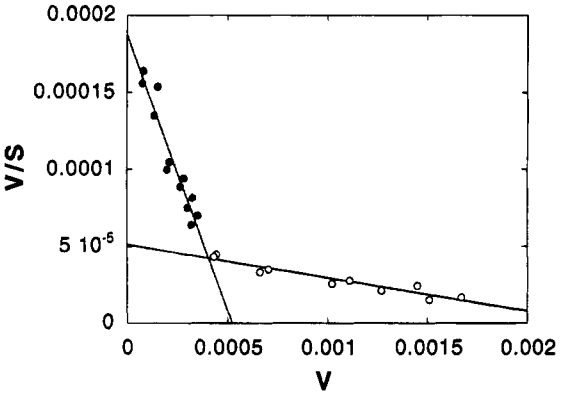

FIGURE 2: Plot of *V/S* versus *V* of DdlB E270Q along with contaminating endogenous wild-type DdlB. The closed circles are ascribed to activity of the wild-type DdlB, and the open circles are for E270Q. The unit of *V* is A_{340}/s; the unit of *S* is mM. The final concentration of the E270Q enzyme in the assay mixture is 0.176 mg/mL. It is estimated that contaminating wild-type enzyme is 1 part in 2000.

indicates a contaminating level of wild-type protein of 0.9/1870 min^{-1} of about 1part in 2000. Subtraction of the wild-type contribution allows confidence that the E270Q mutant does have real residual activity (signal/noise = ca. 4/1) and K_m for D-Ala_2 of 46 mM, clearly distinct from wild-type. Thus a mutant with 0.4% the k_{cat} value of wild-type can be reliably assessed.

ATP Subsite Mutants. In Table 2 the mutants at three subsites (K144, K215, E270) reveal three types of outcomes. Mutation of K144 to either T or A produces an active ligase

Table 3: Kinetic Parameters of the Slow-Binding Inhibition of DdlB Mutants by Phosphinate **1** and ATP

mutants	[D-Ala] (mM)[a]	k_{on} (min^{-1} mM^{-1})	k_{inact} (min^{-1})	K_i/K_{m1} (D-Ala)
WT	20	82.7	62	0.033
E15Q	80	111.9	4.6	0.00036
H63Q	80	35.4	60.6	0.021
K144A	80	14.5	15.4	0.012
S150A	80	178.9	29.6	0.0019
Y216F	80	35.7	87.8	0.03
Y216K	80	30.3	4.4	0.017
S281A	4[b]	0.35	1.4	0.83
L282R	80	19.0	67	0.043

[a] Concentration of D-Ala present in the assays. 5 mM ATP was used in all of the inhibition studies. [b] In the case of S281A, 4 mM D-Ala was used instead of 80 mM to reduce the amount of inhibitor needed.

with k_{cat} down 3−8-fold. The K_m for D-Ala_1 is below 0.3 mM while K_m for D-Ala_2 is up 20−80-fold. This effect may not be readily interpretable since essentially all the Ddl mutants have increased K_m values for D-Ala_2. Notably the K_ms for ATP in K144A and K144T are up some 50-fold (~50 μM to ~2.5 mM) whereas all the D-Ala_1 and D-Ala_2 subsite mutants affect the ATP K_m value at most by 3-fold. By the k_{cat}/K_mATP ratio the K144 mutants are down 100−400-fold compared to wild-type. The E270Q mutant as noted above retains about 0.2% the k_{cat} of wild-type enzyme while its ATP K_m value is only elevated 4-fold. By the k_{cat}/K_m ratio it is 1/2000 as catalytically efficient as wild-type enzyme. The third ATP subsite residue K215 coordinates both the β-P of ADP and the phosphate group of phosphinophosphate **2** and likely coordinates the transferring γ-PO_3^{2-} group in catalysis. The K215E mutant retains no activity above the value for contaminating wild-type enzyme. In crude extracts of K215A and K215R overproducers, there was again no detectable Ddl activity above the 0.05% noise level, expected for the level of contaminating wild-type enzyme.

D-Ala_1 Subsite Mutants. Four mutants to test recognition of the first D-alanine, D-Ala_1, were assessed after purification. E15Q, H63Q, and S150A were each active catalysts while R255A had no detectable activity over background. E15Q has about one-third the k_{cat} of wild-type, H63Q close to wild-type, and S150A actually some 10% higher than k_{cat}. In the three cases K_m for D-Ala_1 is elevated 350−600-fold while K_m for D-Ala_2 is up 40−55-fold. By k_{cat}/K_m D-Ala_2 criteria these enzymes are 50−150-fold less efficient than wild-type enzyme. The side chain of R255 is apparently considerably more important than the other three since it yields no detectable activity.

D-Ala_2 Subsite Mutants. Of the four proposed D-Ala_2 subsite mutants, D257N has no detectable activity above the 0.05% wild-type enzyme contamination level, consistent with the view that this may be of consequence for structure or function. The L282R mutant exchanges a hydrophobic branched side chain for a long cationic one and retains 10% k_{cat}, no effect on ATP K_m, a 20-fold effect on K_m for D-Ala_2, and a 400-fold elevation of D-Ala_1 K_m. The S281A mutant has a modest drop in k_{cat} with a wide range of uncertainty because it is very difficult to saturate the enzyme with D-Alanine. The K_m for D-Ala_1 cannot be deconvoluted, and the K_m for D-Ala_2 is much greater than 100 mM, such that this K_m may be elevated 500-fold, much more than in any other mutant, except Y216K. This is consistent with decreased recognition of D-Ala_2. Finally Y216 mutated either to F216 or K216 retains substantial activity, especially Y216F with 89% the k_{cat} of wild-type and 1/30 the k_{cat}/K_{m2}, arguing against a crucial catalytic function for the tyrosyl OH group, while Y216 could act as a gate for the active site.

Behavior of Ddl Mutants with Slow-Binding Phosphinate Inhibitor. Eight of the DdlB mutant enzymes were analyzed for kinetics of inhibition by phosphinate **1** in the presence of ATP to determine whether time-dependent loss of activity, reflecting formation and slow release of enzyme bound **2**, still occurred. As summarized in Table 3 all eight mutant Ddl enzymes catalyzed phosphoryl transfer to **1** (eq 2) and concomitant autoinactivation due to failure to release **2**. As previously described for wild-type Ddl (Duncan & Walsh, 1988) the inhibition can be analyzed according to eq 3. The

$$E + I \underset{}{\overset{K_i}{\rightleftharpoons}} E \cdot I \underset{k_4}{\overset{k_{inact}}{\rightleftharpoons}} E \cdot I' \qquad \text{net } k_{on} \tag{3}$$

inactivation followed the expected pseudo-first-order kinetics, and pseudo-first-order rate constants at each inhibitor concentration could be calculated. No saturation was observed at the inhibitor concentrations tested, and higher concentrations were not investigated due to the rapidity of inactivation. The k_{inact} reflects the limiting rate constant for E·I undergoing inactivation to form E·I′ (including phosphoryl transfer from γ-P of ATP), while k_{on} is the overall bimolecular rate constant, reflecting the preequilibrum (K_i) and k_{inact}. The K_i of phosphinate **1** inactivating wild-type enzyme in the presence of ATP is 33 nM, approximately 30-fold lower than D-Ala_1's K_m and 30 000 fold lower than that of D-Ala_2. For the eight mutants in Table 3 S150A and S281A are the two outliers for the bimolecular rate constant with S150A two times higher and S281A 300 times lower than wild-type (Figure 3). If k_{inact} is examined, E15Q, Y216K (but not Y216F), and S281A are reduced by 15−20-fold. The very low k_{on} reflects about a 10-fold less efficient K_i for phosphinate **1** binding and reacting with S281A compared to wild-type Ddl.

DISCUSSION

The recent X-ray structure of DdlB with bound ADP and the phosphinophosphate analog **2** of the tetrahedral adduct reaction intermediate that would arise from attack of D-Ala_2 on D-Ala_1-P makes testable predictions about possible roles of side chains in the active site of this bacterial D,D-dipeptide forming enzyme (Fan et al., 1994). It also led to some suggestions about mechanistic distinctions in the homologous VanA that makes not only D-Ala-D-Ala but also D-Ala-D-lactate depsipeptide, the altered cell wall component that when taken forward yields intermediates terminating in D-Ala-D-lactate, not recognized by vancomycin and thereby leading to resistance to the antibiotic vancomycin (Bugg et al., 1991a,b).

To investigate proposed structure/function relationships, we have constructed, overexpressed, and purified mutants at 11 positions in Ddl B that include alterations of side chains in the subsites proposed to interact with the triphosphate moiety of bound ATP and with the NH_3^+ and COO^- substituents of both the first and second D-alanine molecules.

Several of the conclusions derived from initial characterization of the *E. coli* DdlB mutant enzymes for k_{cat} and for

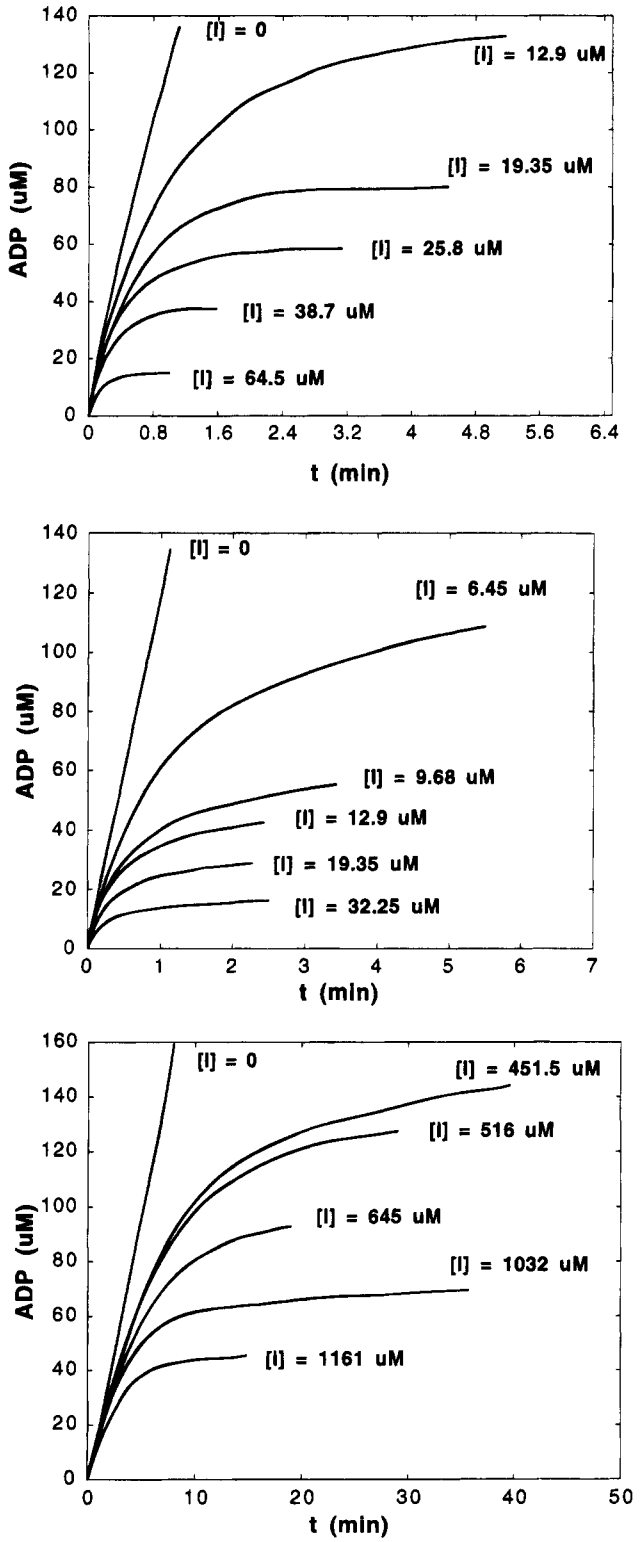

FIGURE 3: Progress curves of DdlB wild type (a, top), S150A (b, middle), and S281A (c, bottom) in the presence of phosphinate inhibitor **1**. The ordinate and abscissa indicate the time course and the formation of ADP during the reaction. The D-Ala concentrations in the assay mixture are 20, 80, and 4 mM, respectively.

ATP and D-alanine K_m values support the predictions about catalysis from the X-ray structure of the enzyme–ADP–phosphinophosphate inhibited complex.

In the ATP binding site the replacement of the K144 side chain by A or T shows a substantial decrease in k_{cat} and a 50-fold effect on ATP K_m, consistent with the proposed role for coordination of the ϵ-NH_3^+ of K144 to one oxygen of the α-PO_3 group of ATP. The replacement of γ-COO^- of E270 by the carboxamide of Q270 reduces V_{max} ca. 250-fold, suggesting a crucial role for bidentate ligation of the E270 γ-COO^- to the Mg^{2+} coordinating the β and γ-PO_3^{2-} of ATP. This coordination presumably orients and shields the negative charge on the γ-PO_3 as it is attacked by the carboxylate of the D-Ala_1 on the way to the first intermediate, the mixed carboxylic phosphoric anhydride D-alanyl$_1$ phosphate.

Another crucial residue in this region of the active site appears to be K215, which as shown in Figure 1 coordinates to both the β-PO_3 of bound ADP (2.86 Å) and the phosphate that has undergone transfer from ATP to the phosphinate oxygen (2.75 Å) to yield the tightly bound phosphinophosphate analog of the tetrahedral adduct **3** that is the second intermediate in catalysis. The NH_3^+ of K215 may have an organizing role and a charge neutralization role in the γ-PO_3 transfer step.

K215 is on an ω-loop (Figure 1b) comprised of residues 205–220 that is thought to swing in and over ATP, D-Ala_1, and D-Ala_2, as these substrates bind. This loop is sensitive to proteolysis in the absence of phosphinate **1** but resistant in the presence of the phosphinate and ATP (Wright & Walsh, 1993). A similar loop protects analogous acyl-P and tetrahedral adducts in the structurally and mechanistically homologous glutathione synthetase (Kato et al., 1994; Tanaka et al., 1993). In Ddl as the loop swings in the key active site, residue K215 is presumably brought into the orientation to bind the ATP triphosphate side chain and assist in setting up the effective geometry for γ-PO_3^{2-} transfer to D-Ala_1. The loop closure will also exclude adventitious water from the active site, preserving the labile acyl-P for capture by the amino group of D-Ala_2.

As D-Ala-D-Ala ligase operates to make the dipeptide D-Ala-D-Ala it utilizes the two chemically identical D-Ala substrate molecules D-Ala_1 and D-Ala_2 in distinct ways, activating D-Ala_1 as an electrophilic acyl phosphate, by the γ-PO_3^{2-} transfer just noted above, and D-Ala_2 as nucleophile to attack the bound acyl-P and produces a tetrahedral adduct as intermediate and then decomposes it to dipeptide product (Scheme 1). The X-ray structure of the phosphinophosphate in Figure 1b suggested the definition of adjacent subsites for the two D-alanine and possible functions for particular enzyme residues for binding, orientation, and protonation state control of each D-Ala at their NH_3^+ and COO^- functional groups to lower the activation barrier.

From the X-ray structure in Figure 1b, in the proposed subsite for D-Ala_1 the following features were tested: (a) the proposed roles of a hydrogen-bonded triad of residues E15, S150, and Y216 (this residue, adjacent to K215, is also brought into the active site by the ω-loop closing over bound substrates and sealing off the active site from bulk solvent; (b) the side chain of R255, which could be in the vicinity of the COO^- of D-Ala_1 when bound; and (c) H63, which is in proximity to the amino and methyl group of D-Ala_1.

The E15–S150–Y216 H-bonded triad could make a direct (or indirect) interaction with the α-NH_3^+ of D-Ala_1. In the event, mutations at E15 or S150 or Y216 do not fatally affect catalysis. There is very little effect on k_{cat} (30%, 120%, 70%), while K_m for D-Ala_1 is elevated from 300–900-fold (but essentially every active mutant has highly elevated K_m for D-Ala_1). It is not yet obvious what side chains if any (or perhaps a coordinated water molecule) are charge pairing with the α-NH_3^+ of D-Ala_1. The R255A mutant, on the other hand, has a k_{cat} which is reduced by at least 3 orders of

Scheme 1

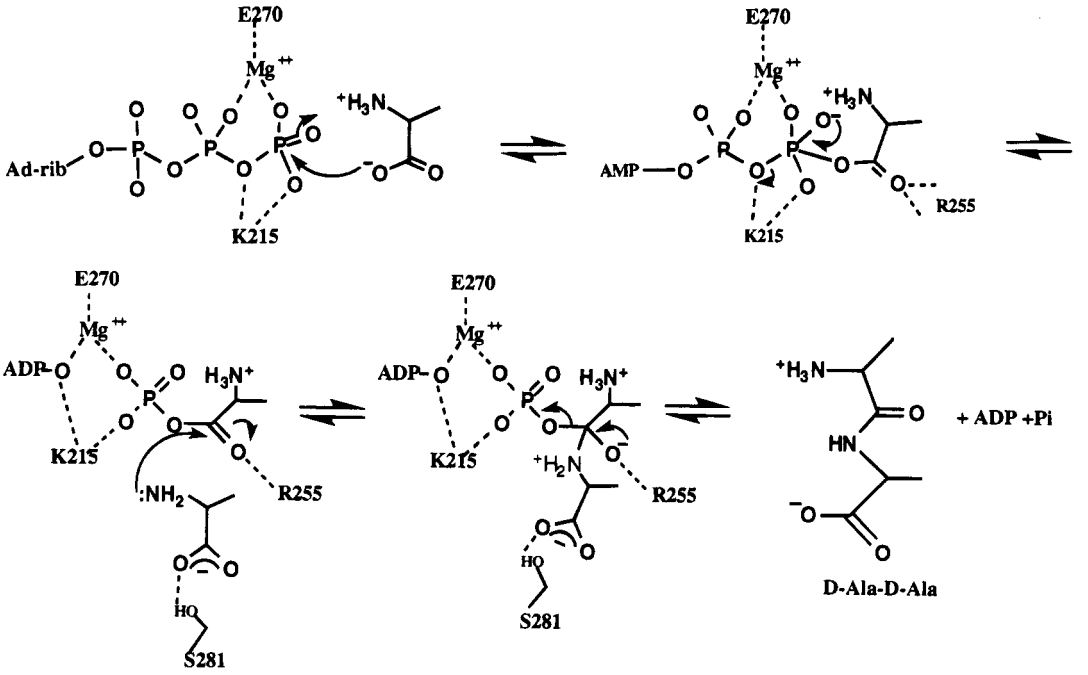

Scheme 2

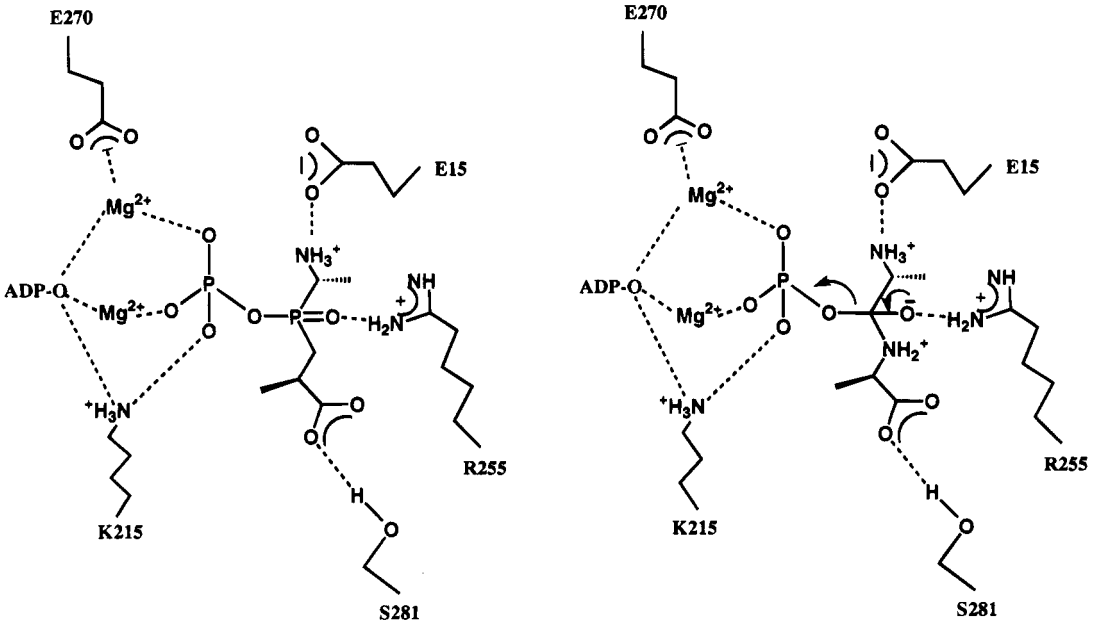

Phosphophosphinate **Tet. intermediate**

2 **3**

magnitude relative to the wild type and is indistinguishable from the trace amount of contaminating wild-type Ddl. This dramatic loss of activity corroborates that the R255 side chain may coordinate the COO^- group of D-Ala_1 on binding and/or the carbonyl oxygen of the COO^- group once bound to orient the $C-O^-$ bond of the COO^- group to attack the γ-PO_3^{2-} of bound ATP. The H63Q mutant retains substantial k_{cat} but has 400-fold elevation of K_m for D-Ala_1. It remains to be seen if H63Q shows loosened specificity in side-chain recognition in the N-terminal amino acid partner in D,D-dipeptide synthesis.

As D-Ala_2 enters the active site, one anticipates recognition of its α-amino and carboxylate by the side chains of residues of the D-Ala_2 subsite and then conversion from the NH_3^+ to NH_2 ionization state to set up attack on the adjacent D-alanyl$_1$ phosphate to yield the tetrahedral adduct **3** that has five charged groups (six net charges) and is mimicked closely by the phosphinophosphate inhibitor **2** (three charged groups, four net charges) (Scheme 2). A major challenge in dissection of the catalytic mechanism of this and other ATP-utilizing, amide-bond-forming ligases such as the architecturally and mechanically homologous GSH synthase (Tanaka et al., 1993) is how formation, stabilization, and decomposition of a tetrahedral structure such as **3** is controlled within the active site.

Inspection of the enzyme−ADP−inhibitor complex as in Figure 1b suggested that the Y216 phenol side chain might be close enough (3.47 Å) to interact with the NH_3^+ in **3** and by extension serve as a catalytic base to yield the free base $:NH_2$ form of D-Ala to initiate formation of **3**. Analogously,

the CH_2OH side chain of S281 could H bond to the COO^- of D-Ala_2. The PO_3^{2-} side chain in **2** and presumably in **3** coordinates to the K215 side chain discussed above. The tetrahedral $-P{=}O$ group in **2** interacts with the guanidinium side chain of R255 and the main-chain NH of Gly276 (not shown). In **3** the corresponding volume would be filled by the tetrahedral $C-O^-$ that would be negatively charged and be electrostatically stabilized by the guanidinium group of R255.

The mutagenesis results show clearly that Y216F and Y216K retain much of the wild-type level of k_{cat} so Y216 cannot be an obligate catalytic base to initial tetrahedral adduct **3** formation. Furthermore, Y216F is still a dipeptide not depsipeptide ligase (no detectable D-Ala-D-lactate formation; data not shown). This result suggests that one should look elsewhere for a catalytic base for this step, and two possibilities arose. The first is that there is no catalytic base for deprotonation of D-Ala_2 and that the species that binds from solution is the free base form. The pH optimum for Ddl is pH 9 (Neuhaus, 1962a). Given a pK_a of 10.5 for the NH_3^+ group, between 1% and 10% of D-Ala would be in the free base form at the pH optimum. In this connection the K_m for D-Ala_2 in wild-type Ddl is about 1200-fold higher (1200 μM vs 1 μM) than the K_m for D-Ala_1, which could reflect such a mole fraction difference. In other words, D-Ala_1 binds as the zwitterion but D-Ala_2 binds as the free amine form. This hypothesis could obtain some support from the reported pH-dependent behavior of the ATP-cleaving, amide-forming glutamine synthetase (Colanduoni et al., 1987) in which it was argued that the NH_3 binds from solution. A second alternative is that an active site water molecule is assisting in α-NH_3^+ group deprotonation. One H_2O which is close to the inhibitor is coordinated to D257. The data of Table 2 show that the D257N mutant is in fact without detectable activity (at least 1000× below wild type). It remains to be seen if the loss of activity in D257N is due to dramatic alteration of active site geometry since D257 is also H bonded to R255 by X-ray analysis, but D257 could be playing a role in α-NH_3^+ deprotonation by the intervening H_2O or in subsequent decomposition of **3** in transferring a proton from NH_2^+ to the departing PO_3^{2-} as **3** decomposes in the forward direction to dipeptide product.

The S281A mutant is the most deleteriously affected (500-fold) in K_m for D-Ala_2. This is consistent with the crystal structure which shows an H-bond between the hydroxyl of S281 and the COO^- of **2**. S281 may indeed be the recognition determinant for COO^- binding of D-Ala_2.

All the mutants that retain significant catalytic activity still phosphorylate the phosphinate **1** and have sufficient interaction energy that the phenomenon of slow binding, especially slow release, holds and all the mutants thereby catalyze their own inactivation. We see differences in k_{inact} which may reflect differences in either the $k_{phosphorylation}$ or the K_i. We have yet to determine k_{off} rates from the mutant Enz−ADP−**2** complexes.

At this juncture the initial results on limited mutagenesis of 11 active site residues have led to validation of some of the predictions for amino acid side-chain functions in D-Ala-D-Ala ligase from the X-ray study on the enzyme−ADP−**2** complex. They set the stage for further study on the relative timing of events in wild-type and mutant enzymes, including formation of D-Ala_1-P, its subsequent capture by D-Ala_2, and its breakdown. The role of ω-loop residues other than K215 and Y216 will also be studied to assess effects on energetics and on uncoupling of γ-PO_3^{2-} transfer from amide bond formation if bulk water can gain access to the active site and compete with D-Ala_2 to capture **3**. The DdlB structure/function results will also serve as a template to interpret mechanistic and mutagenesis results on the 38% homologous VanA and VanB ligases that make the depsipeptide D-Ala-D-lactate, which serves as the altered building block in peptidoglycan biosynthesis and confers clinically significant resistance to the antibiotic vancomycin.

ACKNOWLEDGMENT

We thank Dr. Gerard D. Wright for his contribution of DdlB mutant R255A data, Dr. James R. Knox and Mr. Fan Chan for the crystal structure information of DdlB, and Drs. Bruce Ellsworth and Paul A. Bartlett for the phosphinate inhibitor. We also thank Dr. Greg Kellogg for his help in the computer modeling of D-Ala-D-Ala ligase.

REFERENCES

Bradford, M. M. (1976) *Anal. Biochem. 34*, 248−254.
Bugg, T. D. H., & Walsh, C. T. (1992) *Nat. Prod. Rep. 9*, 199−215.
Bugg, T. D. H., Dutka-Malen, S., Arthur, M., Courvalin, P., & Walsh, C. T. (1991a) *Biochemistry 30*, 2017−2021.
Bugg, T. D. H., Wright, G. D., Dutka-Malen, S., Arthur, M., Courvalin, P., & Walsh, C. T. (1991b) *Biochemistry 30*, 10408−10415.
Colanduoni, J., Nissan, R., & Villafranca, J. J. (1987) *J. Biol. Chem. 262*, 3037-3043.
Daub, E., Zawadzke, L. E., Botstein, D., & Walsh, C. T. (1988) *Biochemistry 27*, 3701−3708.
Duncan, K., & Walsh, C. T. (1988) *Biochemistry 27*, 3709−3714.
Duncan, K., Faraci, W. S. Matteson, D. S., & Walsh, C. T. (1989) *Biochemistry, 28*, 3541−3549.
Dutka-Malen, S., Molinas, C., Arthur, M., & Courvalin, P. (1990) *Mol. Gen. Genet. 224*, 364−372.
Fan, C., Moews, P. C., Walsh, C. T., & Knox, J. R. (1994) *Science 266*, 439−443.
Gale, E. F., Cundliffe, E., Reynolds, P. E., Richmond, M. H., & Waring, M. J. (1981) in *The Molecular Basis of Antibiotic Action*, 2nd ed., John Wiley and Sons, London.
Kahan, F. M., Kahan, J. S., Cassidy, P. J., & Kropp, H. (1974) *Ann. N.Y. Acad. Sci. 235*, 364−386.
Kato, H., Tanaka, T., Yamaguchi, H., Hara, T., Nishioka, T., Katsube, Y., & Oda, J. (1994) *Biochemistry 33*, 4995−4999.
McDermott, A. E., Creuzet, F., Griffin, R. G., Zawadzke, L. E., Ye, Q. Z., & Walsh, C. T. (1990) *Biochemistry 29*, 5767−5775.
Morrison, J. F., & Walsh, C. T. (1987) *Adv. Enzymol. Relat. Areas Mol. Biol. 57*, 201−301.
Neuhaus, F. C (1962a) *J. Biol. Chem. 237*, 778−786.
Neuhaus, F. C (1962b) *J. Biol. Chem. 237*, 3128−3135.
Parsons, W. H., Patchett, A. A., Bull, H. B., Schoen, W. R., Taub, D., Davidson, J., Combs, P. L., Spronger, J. P., Gadebusch, H., Weissberger, B., Valiant, M. E., Mellin, T. N., & Busch, R. D. (1988) *J. Med. Chem. 31*, 1772−1778.
Pitillo, R. F., & Foster, J. W. (1953) *J. Bacteriol. 67*, 53.
Sarkar, G., & Sommer, S. S. (1990) *BioTechniques 8*, 404−407.
Segel, I. H. (1975) in *Enzyme Kinetics*, pp 64−71, Wiley, London.
Tanaka, T., Yamaguchi, H., Kato, H., Nishioka, T., Katsube, Y., & Oda, J. (1993) *Biochemistry 32*, 12398−12404.
Walsh, C. T. (1989) *J. Biol. Chem. 264*, 2393−2396.
Waxman, D. J. (1983) *Annu. Rev. Biochem. 52*, 825−869.
Wilhelm, M. P. (1991) *Mayo Clin. Proc. 66*, 165−170.
Wright, G. D., & Walsh, C. T. (1992) *Acc. Chem. Res. 25*, 468−473.
Wright, G. D., & Walsh, C. T. (1993) *Protein Sci. 2*, 1765−1769.
Zawadzke, L. E., Bugg, T. D. H., & Walsh, C. T. (1991) *Biochemistry 30*, 1673−1682.

BI942311Q